

## INSIGHT INTO ELECTRIC POTENTIAL DISTRIBUTION WITHIN MESOPOROUS TITANIUM DIOXIDE FILMS

Renata SOLARSKA<sup>1</sup>, Robin MORAND<sup>2</sup> and Jan AUGUSTYNSKI<sup>3,\*</sup>

*Département de Chimie Minérale, Analytique et Appliquée, Université de Genève,  
30, quai Ernest-Ansermet, CH-1211 Genève, Suisse; e-mail: <sup>1</sup> renata.solarska@chiam.unige.ch,  
<sup>2</sup> robin.morand@chiam.unige.ch, <sup>3</sup> jan.augustynski@chiam.unige.ch*

Received May 23, 2003  
Accepted August 8, 2003

*Dedicated to Professor Sergio Roffia on the occasion of his retirement.*

Charge transport and potential distribution in mesoporous semiconductor films operating in an electrolyte, especially those composed of TiO<sub>2</sub> nanoparticles, are still the subject of wide debate. Herein we describe a series of experiments, performed under band-gap energy illumination of nanostructured TiO<sub>2</sub> films, intended to shed new light on the actual electric potential profile across such three-dimensional electrode. Our approach stems from quite a general observation that addition of various electron acceptors to a solution containing an efficient hole scavenger (e.g., methanol, formic acid) results in a marked drop of the maximum photocurrent at the mesoporous TiO<sub>2</sub> film electrodes whatever the applied anodic bias might be. We have chosen an electron acceptor, MV<sup>2+</sup> dication, which-due to its negative redox potential, more negative than that of the bottom of conduction band of TiO<sub>2</sub> in acidic media – causes a drop of the photooxidation current only in alkaline but not in acidic solutions of hole scavengers. Measurements of the incident photon-to-current efficiencies as a function of wavelength show that the drop of the photocurrent after the MV<sup>2+</sup> addition, observed in alkaline formate solution extends practically over the whole range of wavelengths. As the optical penetration depth in TiO<sub>2</sub> for the wavelengths close to its band edge is expected to match approximately the chosen film thickness, we can conclude that major part of the electric potential drop in the TiO<sub>2</sub> electrode occurs actually close to the back contact.

**Keywords:** Nanostructured TiO<sub>2</sub> film; Photoanode; Potential distribution; Electron scavenger; Methylviologen; Electrochemistry; Semiconductor films; Nanoparticles; Solar cells.

Successful application of nanostructured TiO<sub>2</sub> films in dye-sensitised solar cells since the nineties has prompted numerous attempts to elucidate the nature of charge transport in such devices<sup>1</sup>. At an early stage of investigation and development of the dye-sensitised cell, it was assumed that due to the small size (in the range of 10–20 nm) of individual TiO<sub>2</sub> particles,

which are unable to withstand any significant electric potential gradient, the electron transport across the nanostructured  $\text{TiO}_2$  film should be dominated by diffusion, driven by the electron concentration gradient<sup>1</sup>. The "electron diffusion model" was largely used as the basis for interpretation of transient photocurrent and intensity-modulated photocurrent spectral measurements, involving the dye-sensitised cell, which were intended to elucidate the charge transport through the nanostructured  $\text{TiO}_2$  film. We showed recently<sup>2</sup> that this approach apparently overlooks the real nature of the nanostructured  $\text{TiO}_2$  photoanode which is a typical three-dimensional electrode with a large porosity (ca 60%) and a thickness (in the range of 10  $\mu\text{m}$ ) that is much larger than the pore sizes and the sizes of individual particles. Like any other three-dimensional electrode, the nanostructured  $\text{TiO}_2$  electrode includes two coincidental (superposed) continua, *i.e.*, an electronically conducting solid matrix (the network of interconnected  $\text{TiO}_2$  nanoparticles) and an ionic conductor (the electrolyte filling of the pores of the nanostructured  $\text{TiO}_2$  film). In a photoelectrochemical cell operating under steady-state conditions, the current enters through the outer photoanode/electrolyte interface as ionic current, starts to be progressively converted, *via* the charge transfer reaction, into the electronic current within the  $\text{TiO}_2$  matrix and reaches the back contact as electronic current. Such a situation is consistent with the electron concentration profile within the  $\text{TiO}_2$  network growing towards the back contact and implies the presence of the electric potential gradient across the whole nanostructured  $\text{TiO}_2$  film<sup>2</sup>. This in turn raises the question of distribution of the electric field within the nanostructured  $\text{TiO}_2$  photoanode, either dye-sensitised or employed as a photocatalyst.

Interestingly, when used as photocatalysts, under band-gap illumination (corresponding to the wavelengths shorter than 400 nm), the mesoporous titanium dioxide films formed on electronically conducting substrates exhibit some features similar to those of suspensions of individual  $\text{TiO}_2$  nanoparticles in solution. In particular, in both cases, the rates of photo-oxidation reactions are strongly affected by the nature of hole and also electron scavengers present in solution<sup>3,4</sup>.

This is reflected by unusually large differences between the saturation photocurrents generated at supported nanocrystalline  $\text{TiO}_2$  films in the presence of irreversibly oxidized effective hole scavengers (such as aliphatic alcohols and carboxylic acids) on the one hand, and those obtained in the oxidation of species being a part of reversible redox couples (*e.g.*,  $\Gamma^-$ , hydroquinone) on the other. Low apparent incident-photon-to-current efficiencies (IPCE's) observed in the latter case are clearly due to the inter-

ception of a part of photogenerated electrons by the oxidized form of the redox couple (*i.e.*,  $I_3^-$ , quinone). Such redox cycling accounts for an effective hole-electron recombination causing a marked decrease in the net photocurrent<sup>3</sup>. We observed systematically that the addition of electron acceptors of this kind to a solution containing an efficient hole scavenger (*e.g.*, methanol, formic acid) leads also to an abrupt drop of the saturation photocurrent at mesoporous  $TiO_2$  film electrodes. Importantly, the latter effect still occurs under a large anodic bias, *i.e.*, when the potential applied to the back contact of the  $TiO_2$  film markedly exceeds the reduction potential of the electron acceptor present in solution. The behaviour of this kind is consistent with the absence in such films of a regular space-charge layer and raises an additional question regarding the actual distribution of the electric potential across the film, *i.e.*, between the back contact and the outer film/solution interface. It is to be recalled, in this connection, that in the case of a bulk n-type semiconductor electrode the surface density of electrons decreases exponentially with the anodic bias. The formation of such a depletion layer, under anodic polarisation, makes virtually impossible any reaction involving conduction band electrons.

Herein we report a series of experiments employing the methyl viologen dication,  $MV^{2+}$ , electron acceptor and either polychromatic or monochromatic illumination of various wavelengths in order to probe the spatial changes of the potential possibly occurring within the mesoporous  $TiO_2$  photoanode. Due to a relatively negative value of its reduction potential ( $E_{0\text{MV}^{2+}/\text{MV}^{2+}} = -0.446\text{ V}$ )<sup>5</sup>, more negative than that of the conduction band edge of  $TiO_2$  in acidic media<sup>6</sup>

$$E_{(\text{cb})} = -0.1 - 0.059 \text{ pH (vs SHE)},$$

but becoming more positive than the latter in alkaline solutions, the methyl viologen dication appears particularly suited to establish a correlation between the onset of the electron-acceptor-induced drop of the photocurrent and the actual quasi-Fermi level of electrons in  $TiO_2$ .

## EXPERIMENTAL

The mesoporous  $TiO_2$  films were formed by attaching P25 nanoparticles, containing *ca* 80% anatase and 20% rutile, 25–30 nm in diameter, surface area of *ca* 55 m<sup>2</sup>/g (Degussa) to the conducting glass support (Libbey Owens Ford, 10  $\Omega$ /square, comprising a 0.5  $\mu\text{m}$  thick overlayer of F-doped  $\text{SnO}_2$ ). The details of the preparation are described elsewhere<sup>3</sup>. The thick-

ness of ca 60% porous  $\text{TiO}_2$  films, annealed at 450 °C, was determined with a Tencor Alpha Step 200 profilometer.

Photoelectrochemical experiments were carried out using a Spectra Physics model 2025-04 argon-ion laser (334.0, 351.1 and 363.8 nm emission lines) equipped with neutral density filters as light source. The wavelength photoresponse (*i.e.*, quantum efficiency of the photocurrent vs excitation wavelength) of the  $\text{TiO}_2$  electrodes was determined using a 500 W xenon lamp (Ushio UXL-502HSO) set in an Oriel Model 66021 housing and a Multispec 257 monochromator (Oriel) with a bandwidth of 4 nm. The distance between the quartz window and the  $\text{TiO}_2$  electrode was ca 20 mm. The absolute intensity of the incident light from the monochromator was measured with a Model 730 A radiometer/photometer from Optronic Lab. The light power was approximately  $660 \mu\text{W cm}^{-2}$  at  $\lambda = 300 \text{ nm}$  and  $1680 \mu\text{W cm}^{-2}$  at  $\lambda = 380 \text{ nm}$ .

The measurements were carried out in a two-compartment Teflon cell equipped with a quartz window, by illuminating the  $\text{TiO}_2$  electrode from the side of the film/solution interface. The cell contained about  $30 \text{ cm}^3$  of carefully deaerated solution. The counter-electrode consisted of a platinum sheet and  $\text{AgCl/Ag/Cl}^-$  was the reference electrode. All potentials are quoted with respect to the standard hydrogen electrode (SHE). The solutions were prepared from reagent grade chemicals and Milli-Q water. Methyl viologen dichloride (puriss. Fluka) was the source of  $\text{MV}^{2+}$  dications.

## RESULTS AND DISCUSSION

As shown in Fig. 1a, the addition of  $\text{MV}^{2+}$  to a 0.1 M aqueous solution of formic acid of ca pH 1 causes, in fact, a perceptible increase in the photocurrent at the mesoporous  $\text{TiO}_2$  photoanode. This effect, enhanced by stirring of the solution, may be assigned to the photooxidative decomposition

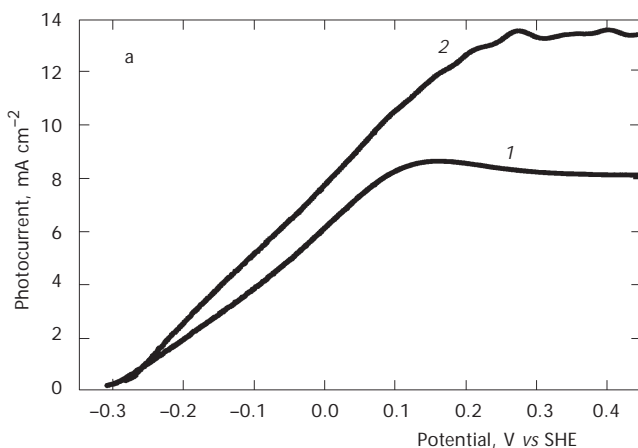


FIG. 1

Effect of a 1 mM  $\text{MV}^{2+}$  addition on photocurrent-voltage behaviour of a ca 2.7  $\mu\text{m}$ -thick mesoporous  $\text{TiO}_2$  photoanode irradiated with argon-ion laser light: a 0.1 M aqueous  $\text{HClO}_4$ /0.1 M  $\text{HCOOH}$  solution

of the  $MV^{2+}$  species occurring in parallel with that of formic acid. It is to be noted that the photooxidation of the  $MV^{2+}$  dications is visibly not adversely affected by the strong positive charge carried by the  $TiO_2$  nanoparticles in the acidic solution (the point of zero charge of P25 powder employed in the present work is close to pH 6). On the other hand, when the formate solution is made alkaline (pH  $\approx$  10) the addition of  $MV^{2+}$  ions

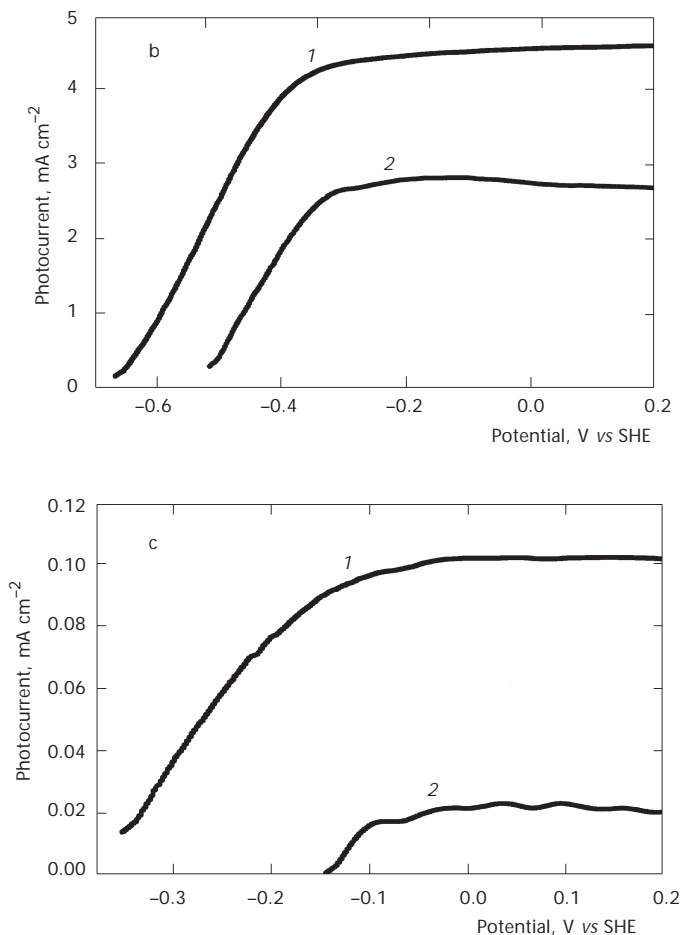
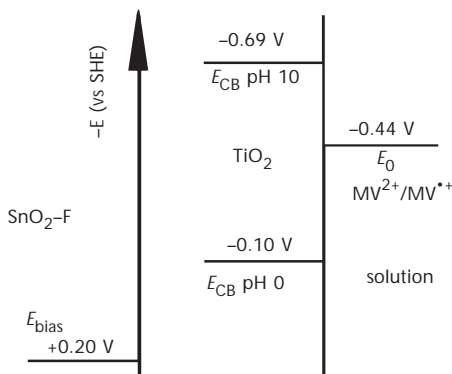


FIG. 1

Effect of a 1 mM  $MV^{2+}$  addition on photocurrent-voltage behaviour of a ca 2.7  $\mu\text{m}$ -thick mesoporous  $TiO_2$  photoanode irradiated with argon-ion laser light: b and c 0.1 M  $NaClO_4$ /0.1 M  $HCOONa$ /borax solution of pH 9.5. Curves 1 and 2 were recorded in the absence (1) and in the presence of  $MV^{2+}$  (2), respectively. The laser power was 200 mW/0.28 cm<sup>2</sup> for a and b and 2 mW/0.28 cm<sup>2</sup> for c

produces a marked drop of the photocurrent. The latter effect (again affected by stirring of the solution) is still more pronounced under low-intensity illumination (*cf.* Fig. 1c) for which the contribution of the electron scavenging process to the total current suffers less from the slow diffusion of  $MV^{2+}$  dications through the pores in the  $TiO_2$  film. These observations prompted us to determine the critical pH at which scavenging of the electrons by the  $MV^{2+}$  species becomes perceptible. Saturation photocurrents, corresponding essentially to the oxidation at  $TiO_2$  of methanol in a solution containing simultaneously  $MV^{2+}$ , were monitored as a function of either increasing or decreasing pH. To minimize local pH changes within the  $TiO_2$  film, medium intensity UV illumination was employed. A clear drop of the saturation photocurrent occurred between pH 7 and 8 and, like in Figs 1b and 1c, was accompanied by a large positive shift of the photocurrent onset potential. At pH 7, at which the  $MV^{2+}$  dications start to intercept the photogenerated electrons, the potential of the conduction band edge of  $TiO_2$  is about  $-0.51$  V vs SHE. This is close to the onset potential of *ca*  $-0.35$  V observed for the reduction of the  $MV^{2+}$  dication (from a 1 mM solution) to the cation radical,  $MV^{+}$ , at glassy carbon and silver electrodes<sup>7</sup>. Clearly, despite a large positive potential applied to the back contact of the photoanode, the actual quasi-Fermi level of electrons, at least in a part of the  $TiO_2$  film, remains, in fact, close to its conduction band edge potential (*cf.* Scheme 1).



SCHEME 1

Schematic diagram of energy levels involved in the scavenging by  $MV^{2+}$  dications of electrons photogenerated at the nanostructured  $TiO_2$  photoanode

In an attempt to probe the potential distribution across the mesoporous film, additional experiments were carried out employing monochromatic illumination of varying wavelengths and, consequently, penetration depths in the film. In Fig. 2b are displayed incident photon-to-current conversion efficiencies (IPCE) for a *ca* 3  $\mu\text{m}$ -thick  $\text{TiO}_2$  film, measured in a 0.1 M formate solution of  $\text{pH} \approx 10$ , in the absence and in the presence of 1 mM  $\text{MV}^{2+}$ .

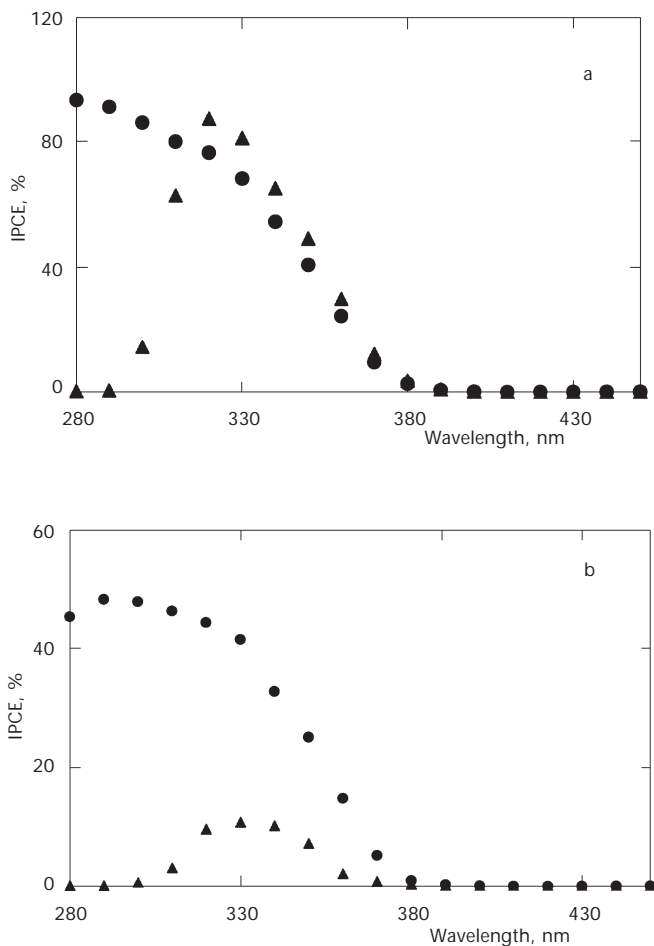


FIG. 2

Spectral responses (*i.e.*, incident photon-to-current conversion efficiencies plotted *versus* wavelength) for a *ca* 3  $\mu\text{m}$ -thick mesoporous  $\text{TiO}_2$  photoanode obtained for a in 0.1 M aqueous  $\text{HClO}_4/0.1$  M  $\text{HCOOH}$  solution; for b in 0.1 M  $\text{NaClO}_4/0.1$  M  $\text{HCOONa}$ /borax solution of  $\text{pH} 9.5$  without (●) and in the presence of 1 mM  $\text{MV}^{2+}$  (▲)

Addition to the solution of methyl viologen leads to a virtual suppression of the photocurrent, in the range of short wavelengths (270–300 nm), which in part can be assigned to the light absorption by  $MV^{2+}$ . In fact, as shown in Fig. 3, the absorbance of the methyl viologen dication, exhibiting a maximum at 255 nm, extends to *ca* 310 nm (1 mM  $MV^{2+}$  solution)<sup>8</sup>. However, the important drop of the photocurrent (and of the IPCE), observed over the whole range of wavelengths absorbed by the  $TiO_2$  film, is clearly consistent with a highly effective withdrawal of the photogenerated electrons by the  $MV^{2+}$  dications. In the absence of more precise data, which would permit to estimate the effect of the film porosity (probably changing across the film) upon its optical properties, it is impossible to set an actual limit of film thickness along which a part of photogenerated electrons continues to be intercepted by methyl viologen. On the other hand, the spectral response recorded in a solution of formic acid of  $pH \approx 1$  containing the  $MV^{2+}$  dications (Fig. 2a) follows first the absorption spectrum of the latter species to reach at 310 nm the regular photoresponse of the  $TiO_2$  film typical of formic acid solution.

The data presented in Fig. 2 clearly indicate that, at least under relatively low-intensity illumination, the quasi-Fermi level of electrons in the  $TiO_2$  film remains close to the actual (pH-dependent) conduction band edge potential of the semiconductor, despite the large anodic bias applied to the back contact. This in turn implies that a major part of the electric potential drop (even if not the whole) in the nanostructured  $TiO_2$  film occurs actu-

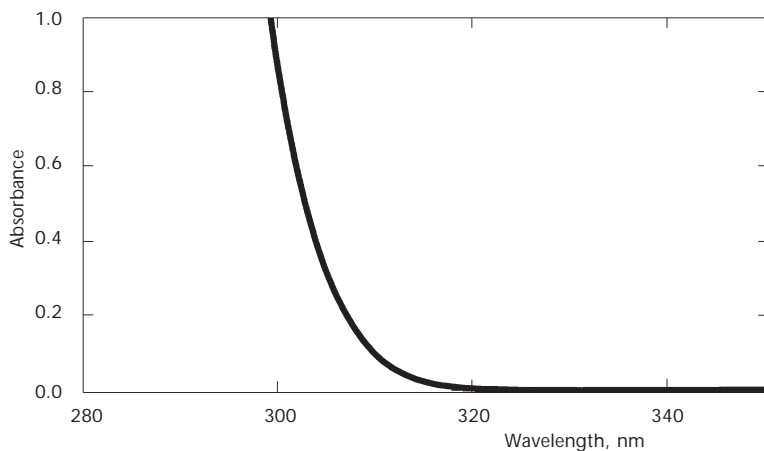


FIG. 3  
Optical absorption spectrum of a 1 mM  $MV^{2+}$  solution; the cell had an optical length of 10 mm



ally close to the back contact, *i.e.*, at the F-SnO<sub>2</sub>/TiO<sub>2</sub> interface. At this point our latter conclusion rejoins with earlier suggestions<sup>9-13</sup> regarding the location of the potential drop in the dye-sensitised TiO<sub>2</sub> photoanode.

*This work was supported by the Swiss National Science Foundation.*

## REFERENCES

1. Hagfeldt A., Grätzel M.: *Acc. Chem. Res.* **2000**, *33*, 269; and references therein.
2. Augustynski J.: *J. Phys. Chem. B*, in press.
3. Wahl A., Augustynski J.: *J. Phys. Chem. B* **1998**, *102*, 7820.
4. Wahl A., Ulmann M., Carroy A., Augustynski J.: *J. Chem. Soc., Chem. Commun.* **1994**, 2277.
5. Ito M., Kuwana T.: *J. Electroanal. Chem. Interfacial Electrochem.* **1971**, *32*, 415.
6. Duonghong D., Ramsden J., Graetzel M.: *J. Am. Chem. Soc.* **1982**, *104*, 2977.
7. Feng Q., Yue W., Cotton T. M.: *J. Phys. Chem.* **1990**, *94*, 2082.
8. Landrum H. L., Salmon R. T., Hawkrigde F. M.: *J. Am. Chem. Soc.* **1977**, *99*, 3154.
9. Schwarzburg K., Willig F.: *J. Phys. Chem. B* **1999**, *103*, 5743.
10. Vanmaekelbergh D., deJongh P. E.: *J. Phys. Chem. B* **1999**, *103*, 747.
11. Pichot F., Gregg B. A.: *J. Phys. Chem. B* **2000**, *104*, 6.
12. Cahen D., Hodes G., Graetzel M., Guillemoles J. F., Riess I.: *J. Phys. Chem. B* **2000**, *104*, 2053.
13. Turrion M., Macht B., Tributsch H., Salvador P.: *J. Phys. Chem. B* **2001**, *105*, 9732.